Effects of geometric nonlinearities on the vibration reduction performance of tuned mass dampers on top of flexible structures

Xiaohui Liu[1], Zhe Qu[1]*, Yuli Huang[2], Akira Wada[3]

1. Key Laboratory of Earthquake Engineering and Engineering Vibration, Institute of Engineering Mechanics, China Earthquake Administration; Key Laboratory of Earthquake Disaster Mitigation, Ministry of Emergency Management, No.1 Chaobai Street, Yanjiao, Sanhe, Hebei 065201, China.
2. Arup, 560 Mission Street, Suite 700, San Francisco, CA 94105, United States.
3. Tokyo Institute of Technology, Nagatsuta, Midori, Yokohama, 226-8503, Japan.
*Corresponding author: Zhe Qu. E-mail: quz@iem.ac.cn

Abstract: A tuned mass damper (TMD) on top flexible structures may sustain considerable rotation because of the significant flexural deformation of the supporting structure. The effects of such rotation on the vibration reduction performance are generally neglected in the analysis and design of TMD-controlled systems, by assuming that the mass moves only laterally in a fixed global coordinate. This technical note critically reviews this assumption by comparing the dynamic responses of a lumped-mass Euler beam with a TMD on top in either fixed or corotational coordinates to harmonic ground excitations. The results show that the corotational local coordinate of TMDs, which introduces geometric nonlinearity into the system, tends to bias the peaks of the frequency response curve toward lower excitation frequency, but such an effect is less profound than that induced by the P-Δ effect, another source of geometric nonlinearity in the system. The relative error in the peak frequency response of neglecting this effect increases for larger lateral drift of the supporting structure and smaller mass ratio of the TMD. An empirical equation for estimating this error is proposed to assist the decision-making of whether this assumption is appropriate for specific applications of TMDs.

Keywords: tuned mass damper, slender structure, corotational coordinate transformation, geometric nonlinearity, frequency response analysis

1 Introduction

Tuned mass dampers (TMDs) have been shown effective in reducing the dynamic response of structures (Cao and Li, 2019, 2022; Elias and Matsagar, 2017; Housner et al., 1997; Soong and Costantinou, 1994; Soong and Spencer, 2002; Wang et al., 2019, 2021). They have been increasingly used in the vibration control of flexible structures of large aspect ratios, like tall buildings, bridge towers, and wind towers under either strong winds or earthquakes (Fig. 1).

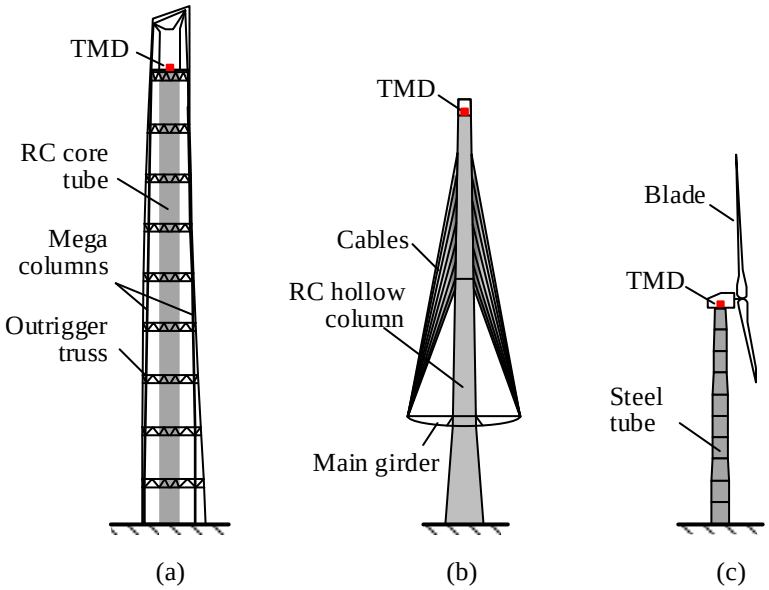

Fig. 1 Typical flexible structures equipped with TMDs: (a) Shanghai Tower (aspect ratio=19, Zhang et al., 2022), (b) tower of Stonecutters' Bridge (aspect ratio=12.4, Guo et al., 2007), and (c) NREL 5-MW baseline wind tower (aspect ratio=15, Chen et al., 2021).

The vibration of such slender structures may exhibit non-negligible geometric nonlinearity due to the large flexural deformation and rotation even if they vibrate within the elastic regime (Pai, 2007). As a primary source of geometric nonlinearity, the *P-Δ* effect accompanying the large drift of flexible structures equipped with TMD under strong winds or earthquakes has been routinely considered by researchers and practitioners in their analyses by performing finite element analysis or finding analytical solutions (Domizio et al., 2015; Hijmissen and van Horssen, 2007; Matta, 2018; Rahman et al., 2021; Wang et al., 2001). The *P-Δ* effect of a shear structure with TMD under proportional internal resonances has also been investigated by Afshar and Amin Afshar (2022) using multiple-scale perturbation method. For TMDs on top of these slender structures, there is another type of geometric nonlinearity that may affect the TMD performance but has been generally ignored. It arises from the rigid-body rotation of the floor plane where the TMD is mounted, as a result of the large flexural deformation of the flexible primary structure [Fig. 2(a)]. In this case, the conventional assumption that the local coordinate of a TMD is always aligned with the global coordinate *X*-*Y* [Fig. 2(b)] does not hold rigorously. Instead, the TMD's local coordinate *x*-*y* rotates together with the rotating floor plane [Fig. 2(c)]. In this paper, we critically review the conventional assumption of neglecting the effect of such a corotational TMD local coordinate by frequency response analyses.

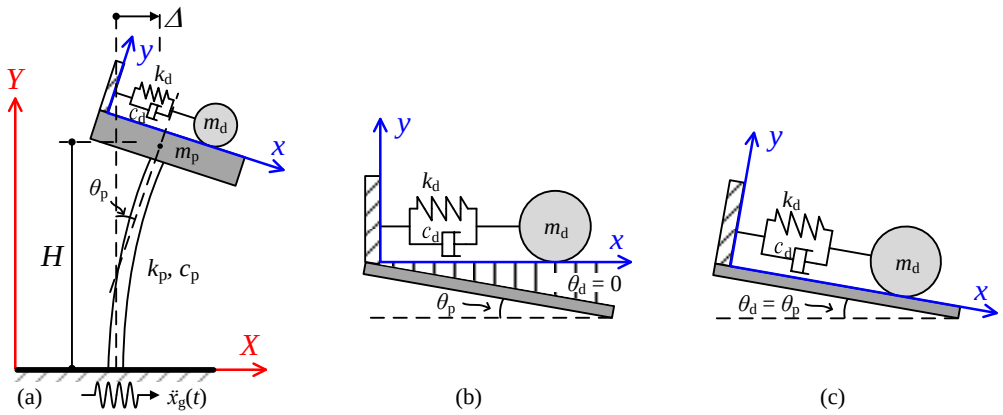

Fig. 2 Coordinate transformation of TMDs: (a) primary structure with TMD in corotational coordinates, (b) TMD in assumingly fixed local coordinates, and (c) TMD in corotational local coordinates.

2 Problem statement and numerical modeling

Take the 2-degree-of-freedom (2DOF) system in Fig. 2(a) as a simple representation of a flexible structure with a TMD on top of it. Its equation of motion under the excitation of ground acceleration $\ddot{x}_g$, when *P*-Δ effect is ignored for simplicity, is:

$$\begin{bmatrix} m_p & 0 \\ 0 & m_d \end{bmatrix}\begin{Bmatrix} \ddot{x}_p \\ \ddot{x}_d \end{Bmatrix} + \begin{bmatrix} c_p + c_d\cos\theta_d & -c_d\cos\theta_d \\ -c_d\cos\theta_d & c_d\cos\theta_d \end{bmatrix}\begin{Bmatrix} \dot{x}_p \\ \dot{x}_d \end{Bmatrix} + \begin{bmatrix} k_p + k_d\cos\theta_d & -k_d\cos\theta_d \\ -k_d\cos\theta_d & k_d\cos\theta_d \end{bmatrix}\begin{Bmatrix} x_p \\ x_d \end{Bmatrix} = -\ddot{x}_g\begin{bmatrix} m_p \\ m_d \end{bmatrix} \tag{1}$$

where k_p, c_p, and m_p are the stiffness, damping coefficient, and mass of the SDOF system that represents the primary structure, respectively; k_d, c_d, and m_d are the stiffness, damping coefficient, and mass of the TMD, respectively; x_p and x_d are the lateral displacement of the primary structure in the global *X*-*Y* coordinate and that of the TMD in its local coordinate *x*-*y*, respectively; $\ddot{x}_g$ is the horizontal ground acceleration; θ_d is the rotation angle of the local coordinate of the TMD [Fig. 2(a)]. $\theta_d = 0$ if the local coordinate of the TMD is assumed to be fixed to the global coordinate [Fig. 2(b)]. Otherwise, when the TMD is installed on top of the primary structure, $\theta_d = \theta_p$, which is the global rotation at the top attributed to the flexural deformation of the primary structure [Fig. 2(c)]. In this case, it introduces geometric nonlinearity to the system even if the *P*-Δ effect of the primary structure is neglected.

Numerical models are established in OpenSees (McKenna, 2011) for the system in Fig. 2(a). The primary structure is represented by a 10-meter-tall cantilever of Euler beam element supporting a lumped mass of 300 kg on top. The cross-section of the cantilever is dimensioned to exhibit a lateral stiffness of 10.8 kN/m, resulting in a circular frequency of $\omega_p = \sqrt{k_p/m_p} = 6$ rad/s. The damping ratio $\xi_p = c_p/(2\omega_p m_p)$ is assumed to be 1%. As a major source of geometric nonlinearity, *Corotational* coordinate transformation is used in the numerical model when the *P*-Δ effect of the primary structure is considered. Otherwise, *Linear* coordinate transformation is used.

The TMD is represented by a lumped mass of m_d connected with the primary structure by two

user-defined *coroZerolength* elements, one with the *Viscous* material for the dashpot and the other with the *Elastic* material for the spring. The *coroZerolength* element is based on the embedded *Zerolength* element in OpenSees. It enables the corotation of the element's local coordinate by updating the geometric transformation matrix according to the current rotation of one of the nodes. This corotation is represented by a non-zero θ_{d} in Eq. 1 and is another source of geometric nonlinearity of the system. The technical details of the used-defined element are provided in Appendix A.

The classical method by Warburton (1982) is adopted to optimize the TMD parameters, i.e., the frequency ratio α and damping ratio ξ_{d} (Eqs. 2 and 3). The results under various mass ratios μ are listed in Table 1. Although more advanced optimal design methods for TMDs (Bakre and Jangid, 2007; Fujino and Abé, 1993; Hoang et al., 2008; Kim and Lee, 2018; Lee et al., 2006; Sadek et al., 1997) also apply, and the optimal parameters may differ depending on the methods, the conclusions hold as long as the geometric nonlinearity of concern is not explicitly considered in the optimization.

$$\alpha = \frac{\omega_d}{\omega_{\mathrm{p}}} = \frac{\sqrt{(1-\mu/2)}}{1+\mu} \tag{2}$$

$$\xi_{\mathrm{d}} = \sqrt{\frac{3\mu}{8(1+\mu)(1-\mu/2)}} \tag{3}$$

where $\alpha = \omega_d/\omega_{\mathrm{p}}$ is the frequency ratio, $\omega_{\mathrm{p}} = \sqrt{k_{\mathrm{p}}/m_{\mathrm{p}}}$ and $\omega_{\mathrm{d}} = \sqrt{k_{\mathrm{d}}/m_{\mathrm{d}}}$ are the circular frequencies of the primary structure and the TMD; $\mu = m_{\mathrm{d}}/m_{\mathrm{p}}$ is the mass ratio; $\xi_{\mathrm{d}} = c_{\mathrm{d}}/(2\omega_{\mathrm{d}}m_{\mathrm{d}})$ is the damping ratio of the TMD.

Table 1. Optimal parameters of TMDs

Mass ratio μ	1%	2%	3%	4%	5%
Frequency ratio α	0.9876	0.9755	0.9636	0.9519	0.9404
Damping ratio ξ_{d}	0.0611	0.0862	0.1053	0.1213	0.1353

Three models of different combinations of the modeling techniques in Table 2 are investigated to distinguish the effect of the geometric nonlinearities from the two different sources. To focus on the effect of geometric nonlinearity in the problem, both the primary structure and the TMD are assumed to exhibit no material nonlinearity.

Table 2. Analysis models

Models	*P-Δ* effect of primary structure	Corotational TMD local coordinate
1	×	×
2	√	×
3	√	√

3 Frequency responses

The frequency responses of the systems are obtained by performing nonlinear time-history analyses and extracting the steady-state peak responses x_{max} of the primary structure to harmonic ground excitation $\ddot{x}_g(t) = a_g \sin \Omega t$, where a_g is the peak ground acceleration, and Ω is the excitation frequency. A non-dimensional dynamic magnification factor, $R = x_{max}/x_{st}$, is defined for ease of comparison, where x_{st} is the static structure response under the static horizontal load of $F = m_p a_g$. Fig. 3 compares the frequency response curves of the systems with various degrees of geometric nonlinearity. Different mass ratios of the TMD and the ground motion amplitudes are considered, while the primary structure remains the same.

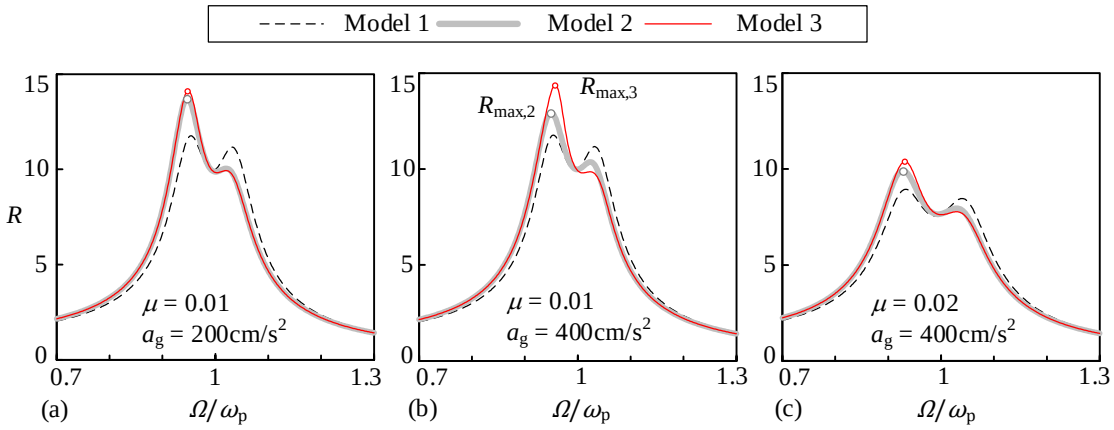

Fig. 3 Frequency responses of dynamic magnification factor R for (a) $\mu = 0.01$, a_g = 200cm/s^2, (b) $\mu = 0.01$, a_g=400cm/s^2, (c) $\mu = 0.02$, a_g=400cm/s^2

For the linear model (Model 1), the frequency response curves of the R-factor exhibit two peaks on both sides of the resonant point of $\Omega = \omega_p$. The R-factors at the peaks are not influenced by the excitation amplitude a_g because the system is linear, while the mass ratio μ of the TMD has a major influence on the peak R-factors. By considering *P-Δ* effect of the primary structure (Model 2), the peak R-factors on the left-hand side of the resonant point ($\Omega < \omega_p$) are raised while the right-hand side ($\Omega > \omega_p$) ones suppressed. The extent of the rise or suppression of the peaks is dependent on the excitation amplitude, indicating the nonlinearity of the system.

The nonlinearity introduced by the corotational local coordinate of the TMD tends to further

bias the frequency response curve of R-factors towards the left-hand side peak. This effect tends to increase with stronger excitation [Fig. 3(a) and (b)], but to decrease with larger mass ratios [Fig. 3(b) and (c)]. The relative difference between the maximum R-factors obtained by Models 2 and 3 is defined in Eq. 4 to quantify such effects. It is denoted as ϵ_{coro} because it describes the relative error introduced by neglecting the corotation of the local coordinate of the TMD. The ϵ_{coro}'s are 2.9%, 10.1%, and 4.5%, for the three cases in Fig. 3(a), (b) and (c) respectively.

$$\epsilon_{\text{coro}} = \frac{R_{\text{max},3} - R_{\text{max},2}}{R_{\text{max},3}} \tag{4}$$

4 Relative error of neglecting the corotation of TMD local coordinate

Since the global P-Δ effect has been well known to the research community, we focus on the effects of corotation of the TMD local coordinate in this study and quantify it by ϵ_{coro}. As suggested in Fig. 3, ϵ_{coro} is dependent on the mass ratio μ and the excitation amplitude a_{g}. In the following parametric analysis, a_{g} is replaced by the steady-state peak drift ratio Δ/H (see Fig. 2) because it is closely related to a_{g}, and more importantly, it uniquely determines the peak tip rotation θ_{p} of the primary structure.

The same analyses as in Section 3 were performed for wider ranges of μ and a_{g}. The mass ratio μ ranges from 0.001 to 0.2, while the excitation amplitude a_{g} from 50 to 400 cm/s^2 by an interval of 50 cm/s^2. The corresponding steady-state drift ratio Δ/H is from 0.005 to 0.147 for all cases in the following analyses (data points having Δ/H more than 0.15 are eliminated). Fig. 4 plots the relative error ϵ_{coro} for different combinations of μ and Δ/H. Generally, the effect of the corotational local coordinate of TMDs diminishes for larger μ but increases with the increase of Δ/H.

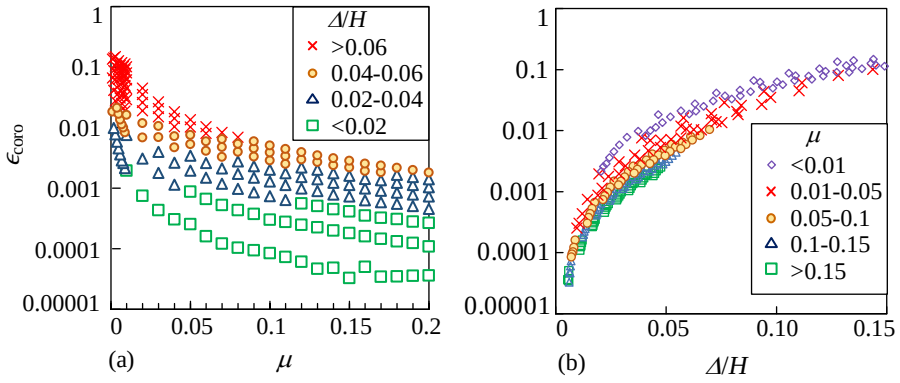

Fig. 4 (a) ϵ_{coro} vs. μ; (b) ϵ_{coro} vs. Δ/H.

All the data points in the current analyses seem to lie on a smooth surface in the 3-dimensional space of μ-Δ/H-ϵ_{coro} [Fig. 5(a)]. The surface can be well described by the function in Eq. 5, which estimates the relative error of neglecting the corotational local coordinate of TMDs ϵ_{coro} by the mass ratio μ and the maximum drift ratio Δ/H of the system. The surface is superimposed in Fig. 5(a) to show its close fit with the data. The estimated ϵ'_{coro} is compared with the true error of ϵ_{coro} in Fig. 5(b). Their root mean squared error is as small as 2.37×10^{-3}.

$$\epsilon'_{\text{coro}} = 1.44 \cdot \frac{(\Delta/H)^2}{\mu^{0.27}} \tag{5}$$

For the seismic design of most engineering structures, the limit drift ratio under the maximum considered earthquake is practically no greater than 2%. At this level of drift ratios, the error of ϵ'_{coro} is only 0.37% for a considerably small mass ratio μ=0.1% as per Eq. 5, which is appropriate to neglect. Although impractical for most civil engineering applications, the error increases rapidly with the increase in the drift ratio. At 5% drift, the error of ϵ'_{coro} is 2.3% as per Eq. 5 for the same mass ratio. In more extreme scenarios, the relative error of ϵ'_{coro} can approach 10% for systems with a TMD of 0.1% mass ratio and exhibiting a greater-than-10% drift ratio. Only in such extreme cases, the geometric nonlinearities may play a nonnegligible role.

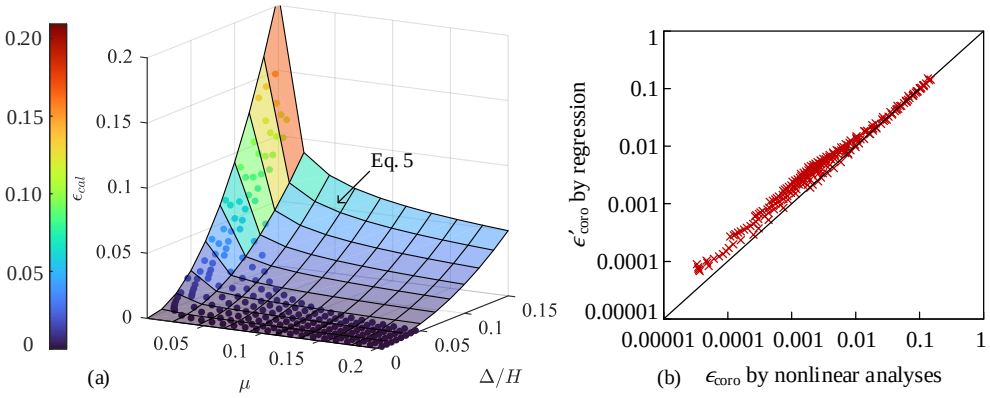

Fig. 5 (a) Comparison of ϵ_{coro}'s and Eq. 5 in μ-Δ/H-ϵ_{coro} space; (b) ϵ_{coro}'s vs ϵ'_{coro}'s.

The negligible effect of such geometric nonlinearity is further demonstrated through the displacement responses of the primary structure of the three models in Table 2 to the seismic excitation of the NS component of the 1940 El Centro record (Fig. 6). The *PGA* of the excitation is scaled up to 2*g* to represent a very strong motion. The mass ratio of the TMD is set to be 1%. The results show that the absolute error in the maximum displacement response is only 1.58mm between Models 1 and 2, and is only 0.0024mm between Models 2 and 3. The relative error between Models 1 and 2 and that between Models 2 and 3 are only 1.65% and 0.00265%, respectively.

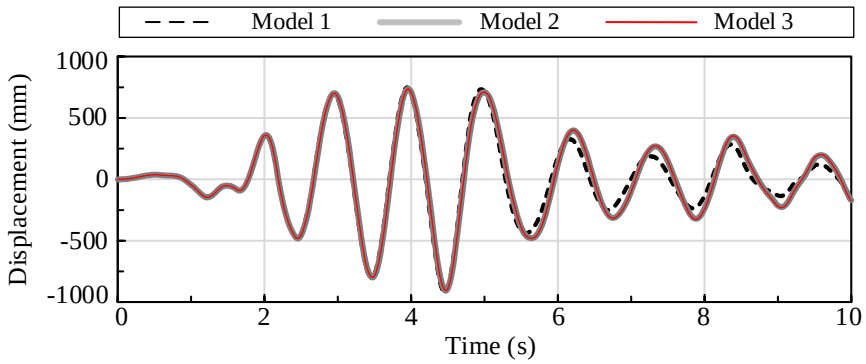

Fig. 6 Displacement response of 3 models under NS component of the 1940 El Centro record

5 Conclusions

This paper critically assesses the effect of neglecting the corotation of the local coordinates of TMDs that slide on the top floor plane of flexural structures. A relative error is defined based on the peak frequency responses of geometrically nonlinear systems to quantify this effect. The results show that both the *P-Δ* effect and the corotational local coordinates of TMDs, the two sources of geometric nonlinearity, tend to amplify the peak frequency response of a system equipped with a TMD that is optimally designed by the fixed-point theory, although the effect of the latter is less profound. Parametric analyses show that the effect of the corotational TMD local coordinate diminishes for a larger mass ratio μ but increases with the increase of the drift ratio *Δ/H*. The error can approach 10% for systems of small mass ratios and exhibiting large drift ratios. An empirical equation for estimating this error is proposed to assist the decision-making of whether the corotation of the local coordinates of TMDs is appropriate to neglect. It's worth mentioning that Eq.5 is assessed for a Euler beam primary structure without any shear deformation. If the deformation of primary structure consists of both shear and flexural components, the rotation angle will be less under the same level of drift ratio, and consequently the effect of the corotational coordinates of TMDs would further decrease, leading to an even smaller ϵ_{coro} than that estimated by Eq.5.

Appendix A. Pseudo-code of user-defined *coroZerolength* element

for each update of the *coroZreolength* element

get rotation angle θ_d

calculate coordinate transformation matrix `transformation`

$$transformation = \begin{bmatrix} \cos\theta_d & \sin\theta_d & 0 \\ -sin\theta_d & \cos\theta_d & 0 \\ 0 & 0 & 1 \end{bmatrix} \tag{A1}$$

calculate transformation matrix `tran`

$$tran = [-transformation \quad transformation] \tag{A2}$$

Funding

The author(s) disclosed receipt of the following financial support for the research, authorship, and/or publication of this article: This work was sponsored by the Natural Science Foundation of China [Grand No. 52122811].

Declaration of Conflicting Interests

The author(s) declared no potential conflicts of interest with respect to the research, authorship, and/or publication of this article.

References

Afshar D and Amin Afshar M (2022) Nonlinear dynamic P-delta interaction between TMD and the frame structure under proportional internal resonances. *Structural Control and Health Monitoring*. DOI: 10.1002/stc.3082.

Bakre SV and Jangid RS (2007) Optimum parameters of tuned mass damper for damped main system. *Structural Control and Health Monitoring* 14(3): 448–470. DOI: 10.1002/stc.166.

Cao L and Li C (2019) Tuned tandem mass dampers-inerters with broadband high effectiveness for structures under white noise base excitations. *Structural Control and Health Monitoring* 26(4): e2319. DOI: 10.1002/stc.2319.

Cao L and Li C (2022) A high performance hybrid passive base-isolated system. *Structural Control and Health Monitoring* 29(3). DOI: 10.1002/stc.2887.

Chen Y, Jin X, Liu H, et al. (2021) Large scale wind turbine TMD optimization based on Blade-Nacelle-Tower-Foundation Coupled Model. *Ocean Engineering* 239: 109764. DOI: 10.1016/j.oceaneng.2021.109764.

Domizio M, Ambrosini D and Curadelli O (2015) Performance of tuned mass damper against structural collapse due to near fault earthquakes. *Journal of Sound and Vibration* 336: 32–45. DOI: 10.1016/j.jsv.2014.10.007.

Elias S and Matsagar V (2017) Research developments in vibration control of structures using passive tuned mass dampers. *Annual Reviews in Control* 44: 129–156. DOI: 10.1016/j.arcontrol.2017.09.015.

Fujino Y and Abé M (1993) Design formulas for tuned mass dampers based on A perturbation technique. *Earthquake Engineering & Structural Dynamics* 22(10): 833–854. DOI: 10.1002/eqe.4290221002.

Guo A, Xu Y and Li H (2007) Dynamic performance of cable-stayed bridge tower with multi-stage pendulum mass damper under wind excitations — I: Theory. *Earthquake Engineering and Engineering Vibration* 6(3): 295–306. DOI: 10.1007/s11803-007-0747-x.

Hijmissen JW and van Horssen WT (2007) On aspects of damping for a vertical beam with a tuned mass damper at the top. *Nonlinear Dynamics* 50(1–2): 169–190. DOI: 10.1007/s11071-006-9150-9.

Hoang N, Fujino Y and Warnitchai P (2008) Optimal tuned mass damper for seismic applications and practical design formulas. *Engineering Structures* 30(3): 707–715. DOI: 10.1016/j.engstruct.2007.05.007.

Housner GW, Bergman LA, Caughey TK, et al. (1997) Structural Control: Past, Present, and Future. *Journal of Engineering Mechanics* 123(9): 897–971. DOI: 10.1061/(ASCE)0733-9399(1997)123:9(897).

Kim S-Y and Lee C-H (2018) Optimum design of linear multiple tuned mass dampers subjected to white-noise base acceleration considering practical configurations. *Engineering Structures* 171: 516–528. DOI: 10.1016/j.engstruct.2018.06.002.

Lee C-L, Chen Y-T, Chung L-L, et al. (2006) Optimal design theories and applications of tuned mass dampers. *Engineering Structures* 28(1): 43–53. DOI: 10.1016/j.engstruct.2005.06.023.

Matta E (2018) Lifecycle cost optimization of tuned mass dampers for the seismic improvement of inelastic structures. *Earthquake Engineering & Structural Dynamics* 47(3): 714–737. DOI: 10.1002/eqe.2987.

McKenna F (2011) OpenSees: A Framework for Earthquake Engineering Simulation. *Computing in Science & Engineering* 13(4): 58–66. DOI: 10.1109/MCSE.2011.66.

Pai PF (2007) *Highly Flexible Structures: Modeling, Computation, and Experimentation*. Reston ,VA: American Institute of Aeronautics and Astronautics. DOI: 10.2514/4.861925.

Rahman M, Nahar T and Kim D (2021) Effect of Frequency Characteristics of Ground Motion on Response of Tuned Mass Damper Controlled Inelastic Concrete Frame. *Buildings* 11(2):

74. DOI: 10.3390/buildings11020074.

Sadek F, Mohraz B, Taylor AW, et al. (1997) A method of estimating the parameters of tuned mass dampers for seismic applications. *Earthquake Engineering & Structural Dynamics* 26(6): 617–635. DOI: 10.1002/(SICI)1096-9845(199706)26:6<617::AID-EQE664>3.0.CO;2-Z.

Soong TT and Costantinou MC (eds) (1994) *Passive and Active Structural Vibration Control in Civil Engineering*. CISM International Centre for Mechanical Sciences. Vienna: Springer Vienna. DOI: 10.1007/978-3-7091-3012-4.

Soong TT and Spencer BF (2002) Supplemental energy dissipation: state-of-the-art and state-of-the-practice. *Engineering Structures* 24(3): 243–259. DOI: 10.1016/S0141-0296(01)00092-X.

Wang A-P, Fung R-F and Huang S-C (2001) Dynamic analysis of a tall building with a tuned-mass-damper device subjected to earthquake excitations. *Journal of Sound and Vibration* 244(1): 123–136. DOI: 10.1006/jsvi.2000.3480.

Wang W, Hua X, Chen Z, et al. (2019) Modeling, simulation, and validation of a pendulum-pounding tuned mass damper for vibration control. *Structural Control and Health Monitoring* 26(4): e2326. DOI: 10.1002/stc.2326.

Wang W, Yang Z, Hua X, et al. (2021) Evaluation of a pendulum pounding tuned mass damper for seismic control of structures. *Engineering Structures* 228: 111554. DOI: 10.1016/j.engstruct.2020.111554.

Warburton GB (1982) Optimum absorber parameters for various combinations of response and excitation parameters. *Earthquake Engineering & Structural Dynamics* 10(3): 381–401. DOI: 10.1002/eqe.4290100304.

Zhang Q, Luo X, Ding J, et al. (2022) Dynamic response evaluation on TMD and main tower of Shanghai Tower subjected to Typhoon In-Fa. *The Structural Design of Tall and Special Buildings* 31(9). DOI: 10.1002/tal.1929.